Nucleation of Polypropylene Crystallization by Single-Walled Carbon Nanotubes

ARTICLE *in* THE JOURNAL OF PHYSICAL CHEMISTRY B · MAY 2002

Impact Factor: 3.3 · DOI: 10.1021/jp014622y

Nucleation of Polypropylene Crystallization by Single-Walled Carbon Nanotubes

Brian P. Grady,* Francisco Pompeo, Robert L. Shambaugh, and Daniel E. Resasco

Department of Chemical Engineering and Materials Science, The University of Oklahoma, Norman, Oklahoma 73019

Received: December 20, 2001; In Final Form: March 28, 2002

Nonisothermal and isothermal crystallization experiments were performed on polypropylene mixed with carbon nanotubes produced by disproportionation of CO on Co−Mo catalysts. Functionalization of the nanotubes with octadecylamine made the tubes hydrophobic and allowed the tubes to be solubilized in an organic solvent. Mixing of the nanotubes with the polymer was accomplished by adding the nanotubes to a Decalin solution that contained dissolved polypropylene, followed by evaporation of the solvent. Dynamic mechanical analysis indicated very little difference in the small-strain mechanical properties between filled and unfilled polymers at the very low solid levels that were tested. By contrast, the crystallization behavior of the filled and unfilled polymer was quite different. Nanotubes promoted growth of the less-preferred beta form of crystalline polypropylene at the expense of the alpha form. In nonisothermal crystallization, the total amount of crystalline material in the sample was the same for the filled and unfilled materials. However, for isothermal crystallization experiments, the percent crystallinity in the filled materials was slightly higher. Most importantly, the rate of crystallization was substantially higher in the filled system. The results presented in this paper clearly show that carbon nanotubes nucleate crystallinity in polypropylene.

1. Introduction

The unusually high Young's modulus and tensile strength coupled with the low density of single-walled nanotubes (SWNT) have prompted investigations of these materials as reinforcement in polymer composites.[1] Of course, the effective utilization of SWNT as reinforcement materials is not only related to their intrinsic properties but also to characteristics such as dispersion, alignment, and interfacial properties.[2] In our laboratory, we have been particularly interested in carbon nanotubes as reinforcing fillers for thermoplastics. One unique aspect of nanotubes is that they can retain a high aspect ratio even when processed as melt-spun fibers, unlike typical micron diameter fillers. The resultant morphologies in this situation, especially in the case where the filler can nucleate crystallinity, might be totally unique.

Carbon fibers, which are closely related to carbon nanotubes, can nucleate crystallinity in isotactic polypropylene.[3−9] This nucleating ability leads to transcrystallization, which is a region of highly oriented crystalline material with the *c*-axis parallel to the fiber surface at regions very close to the fiber surface.[10] This orientation is a result of very dense nucleation on the fiber, which consequently restricts crystal growth in the direction normal to the fiber. However, several studies have shown that the crystalline growth rate, that is, the rate of the crystal front movement independent of nucleation, is no different for a transcrystalline layer versus a normal spherulite.[5,9]

The fundamental morphological characteristics of the carbon fiber that lead to the formation of this transcrystalline layer have not been established. Thomason and Van Rooyen[9] showed that high modulus (HM) carbon fibers tend to form transcrystalline layers with isotactic polypropylene, while high-strength (HS) fibers tend to not form transcrystalline layers. A similar distinction was found for syndiotactic polystyrene transcrystallinity.[11] HM fibers can be produced from either polyacrylonitrile (PAN) or pitch, while the HS fibers are typically only produced from PAN. However, there is not enough evidence to conclude that only pitch-based fibers can cause transcrystallinity. In a second paper by Thomason and Van Rooyen,[12] the authors suggested that transcrystallinity is due to stress between the fiber and the matrix, and hence large differences in axial thermal expansion coefficients between the fiber and the polymer favor transcrystallinity. A similar explanation with some quantification was proposed by another set of authors.[13] However, both sets of authors note that fiber-melt interaction does seem to be important. In the particular case of carbon fibers, the fact that some carbon fibers form transcrystalline layers and others do not would suggest that the interaction between the polymer and the fiber surface is almost certainly important. Sizings (proprietary coatings often applied to fibers to improve processing characteristics or fiber-matrix compatibility) may also play a role. For glass fibers, different sizings have been shown to affect the ability of the fiber to nucleate crystallinity.[14,15]

Clearly, the characteristics required to induce transcrystallinity have not been established. Even if a priori such a prediction could be made for carbon fibers, the specific relevance to carbon nanotubes would not be clear. Hence, the only way to determine whether nanotubes will nucleate crystallinity is through experimental measurement. The purpose of this study is to determine whether carbon nanotubes nucleate crystallization in polypropylene.

2. Experimental Section

2.1 Materials. The SWNT used in this work have been obtained by a catalytic decomposition method based on the disproportionation of CO over Co−Mo/SiO_2 catalysts at a total pressure of 5 atm and 1123 K. In a previous study,[16] we fully characterized the structure and chemical state of these catalysts by EXAFS, XANES, UV/vis-DRS, H_2 TPR, XPS, and DRIFTS

* To whom correspondence should be addressed.

10.1021/jp014622y CCC: $22.00
Published on Web 05/21/2002

of adsorbed NO. The selectivity of the Co−Mo catalysts toward SWNT strongly depends on the stabilization of Co species in a nonmetallic state before exposure to CO, which results from an interaction with Mo. Only those catalysts in which Co is fully stabilized by Mo result in selective production of SWNT. Otherwise, large Co clusters are formed which produce nonselective forms of carbon (MWNT, filaments, graphite, etc.). The SWNT produced by this catalytic method are of a quality comparable to the products obtained by the arc discharge and laser ablation methods. By a temperature-programmed oxidation method previously described,[17] we have determined that the selectivity of the SWNT was above 80% (grams of SWNT/gram of carbon deposit).

The first step in the purification of the SWNT was the elimination of the amorphous carbon, which was accomplished by calcination in air at 573 K for 2 h. The second step was the elimination of the silica support. In this step, 1 g of the material was suspended in a 0.2 M NaOH solution while stirring for 24 h at 338 K. After filtering through a 0.2-μm Teflon-PTFE membrane, the remaining solid was washed with deionized water until the pH was neutral. The solid was then dried overnight at room temperature inside a desiccator. The third step was the elimination of the metals (Co and Mo). This was accomplished by an acid attack in reflux of 2 M nitric acid until the evolution of NO_2 vapors subsided. Again, the solid part was filtered and washed as before. The fourth step was the protonation of the groups generated during the acid attack, which was accomplished by suspending the SWNT in an aqueous solution of HCl, followed by filtering and washing.

The resulting product was characterized by TEM, SEM, XPS, DRIFTS, and Raman spectroscopy. This characterization demonstrated a high quality of the purified SWNT. The tube diameter as determined by Raman spectroscopy and TEM ranged from 0.8 to 1.2 nm. The presence of carboxylic groups in the SWNT was clearly observed by XPS and DRIFTS. These were the only functional groups detected after the purification treatment, contrasting with previous reports that indicated that purified SWNT also contained quinones and ester groups.[18,19] The presence of these carboxylic groups is important in the subsequent functionalization and solubilization. As shown by Chen et al.,[20] it is possible to solubilize SWNT in organic media by a simple functionalization routine. In the first step of this routine, the purified SWNT are contacted with thionyl chloride dissolved in 2-methyl furan to generate an acid chloride in each of the carboxylic groups. In the next step, a long-chain amine is reacted with the acid chloride to form an amide bond and functionalize the SWNT. For our experiments, we used octadecylamine (ODA), which was contacted with the SWNT at 383 K for 96 h.

The product of this step was vacuum-dried at room temperature and then solubilized in Decalin. The term "solubilized" is used in the sense that was used by Chen et al.;[20] the term "colloidal dispersion" is a more accurate representation of the thermodynamic state for the system. The resulting solution was ultracentrifuged at 5000 rpm for 20 min. The very small amount of sediment obtained was due to the non-SWNT carbon in the sample. The presence of SWNT in solution was confirmed by the presence of absorption bands at 530 and 700 nm in the UV−vis spectra; a result expected for metallic and semiconducting SWNT, respectively, in the range of nanotubes diameters observed by TEM.[21]

Fina Dypro isotactic polypropylene pellets with an MFR of 88, a weight average molecular weight of 165 000 g/mol, and a polydispersity of 4 were dissolved in Decalin at 343 K. The previously prepared solution containing the required amount of SWNT was then added to the polypropylene solution. Enough SWNT were added to produce either a 0.6 wt % or 1.8 wt % concentration (on the basis of a solvent-free mixture of the SWNT and the polymer). The resulting solution was stirred with ultrasound (40 kHz) for 30 min. Subsequently, the solvent was evaporated at atmospheric pressure and room temperature for 72 h; further solvent removal was accomplished by placing the sample in a vacuum oven at room temperature for 96 h.

The material produced was in the form of a poorly formed solid with a powdery consistency. This material was then heated above the melting point of polypropylene on a hot plate, and very light pressure was applied via a glass cover slip. The material was slowly cooled to room temperature. Films for dynamic mechanical thermal analysis and differential scanning calorimetry were cut from this approximately 0.5-mm thick material. The thickness was not totally uniform in each sample; variations of up to 20% were common. The average thickness of the particular sample was used as the thickness in the calculation of the moduli. The samples were cut to a 30 mm × 5 mm size for measurement of the dynamic mechanical properties.

2.2 Dynamic Mechanical Thermal Analysis (DMTA). A Solids Analyzer RSA II (Rheometric Scientific) was used to measure storage and loss moduli as a function of temperature. A film and fiber fixture was used to mount the samples, and 3 K temperature steps were used. All experiments were performed with a 10 Hz frequency, 0.1% strain, and with static force tracking dynamic force.

2.3 Differential Scanning Calorimetry (DSC) Experiments. DSC experiments were conducted using a Perkin-Elmer DSC II differential scanning calorimeter with a computerized data acquisition system developed at the University of Oklahoma. Tin and indium were used as temperature calibration standards, and the heating rate was 5 K/min. Given the accuracy by which the calibration was done, coupled with small drifts noticed during a run, the maximum error in temperature is estimated at ±0.5 K. Aluminum sample pans (Perkin-Elmer) with approximately 3-mm diameter bottoms were used for all samples. Liquid nitrogen was used as the heat sink for all experiments.

At the start of a cycle, samples were maintained at 473 K for 5−10 min to completely melt the sample and erase any previous thermal history. This temperature was chosen because 473 K is above the commonly accepted equilibrium melting point for polypropylene.[22] For nonisothermal crystallization experiments, the sample was cooled at the specified rate until the material crystallized. Shortly after crystallization occurred and because further addition of liquid nitrogen was required, the material was then quickly cooled to 313 K to prevent possible annealing. When the instrument was ready, the material was quickly heated to 393 K, a scan at 5 K/min was initiated, and the melting endotherm was measured. The material was then heated to 473 K and the cycle repeated for the next cooling rate.

The same samples were used for both nonisothermal and isothermal crystallization experiments. For the latter test, the first step in the cycle was to maintain a temperature of 473 K for 5−10 min to erase any thermal history. The temperature was first reduced to 443 K and the instrument was allowed to reach thermal equilibrium (which required approximately 20 s and was independent of sample), at which time the temperature was lowered to the crystallization temperature. The cooling rate for both steps was nominally 320 K/min. The sample was maintained at the crystallization temperature until the signal was

flat, indicating that crystallization was complete. 443 K was used instead of 473 K to reduce the time required for cooling; however, since no measurable crystallization occurred at the former temperature, this choice should not affect results presented in this paper. The time $t = 0$ was assumed to be the time at which cooling began. The time difference between the start of cooling and the end of cooling according to the temperature displayed on the instrument was less than 3 s. This cycle was then repeated for the next crystallization temperature.

The percent crystallinity $\chi(t \text{ or } T)$ as a function of time, t, or temperature, T, for a sample of known polymer mass, m_p, was determined by eq 1.

$$\chi(t \text{ or } T) = \frac{A(t \text{ or } T) \times r \times 100}{\Delta H^0_f \times m_p \times f} \quad (1)$$

The DSC range setting in cal/min is represented by r, and f is the DSC calibration constant determined from the indium crystallization peak. The area under the crystallization or melting curve, $A(t \text{ or } T)$ was determined by numerically integrating the baseline-subtracted DSC output over the time or temperature range in which the sample crystallizes or melts. In isothermal crystallization experiments, the relative crystallinity, $\chi_r(t)$, was determined from the area normalized to the total area. The value of the heat of melting for pure crystalline polypropylene, ΔH^0_f, was assumed to be 146.5 J/g.[23]

Isothermal crystallization data were fit to the Avrami equation, Equation 2, with the SPSS Inc. software package, SigmaPlot, which uses the Marquardt−Levenberg algorithm for least-squares minimization. The Avrami equation is a semiempirical expression where nucleation and linear growth rates are embodied in the crystallization rate constant, K, and the dimensionality is characterized by the Avrami exponent, n,

$$\chi_r(t) = 1 - e^{-K(t-\tau o)n} \quad (2)$$

The Avrami exponent is rarely a whole number and is a function of both the nucleation mechanism and the dimensionality of growth, so it is not possible to fully determine the dimensionality from kinetic data alone. Some commonly accepted guidelines state that n varies from 1 to 4 and broadly describes dimensionality as the regions from 1 to 2, 2 to 3, and 3 to 4, which generally indicate 1, 2, and 3-dimensional growth, respectively. The exponential term contains $(t-\tau_o)$ instead of the normal t because $t = 0$ was taken to be the time when cooling started. Clearly cooling is not instantaneous, however, the value of τ_o was much larger than the cooling time and an induction time for crystallization was also present. As a result, three parameters, n, K, and τ_o, were allowed to float when eq 2 was fit to the data. The lower value of the percent crystallinity was set to $\chi_r = 5\%$ to reduce the problem of imprecise baseline location. The upper value of the percent crystallinity used in the fit was determined by the point where the values of the fitted parameters did not vary, which was determined experimentally to be 75% relative crystallinity.

3. Results and Discussion

Dynamic mechanical spectra are shown in Figure 1. Only very small differences existed between the small-strain mechanical response of the polymer with and without nanotubes. This result is much different from the one reported for polypropylene filled with 100-nm diameter carbon fibers grown from vapor.[24] In this previous study, the addition of 2 wt % carbon fibers caused the storage modulus (E′) at room temperature to increase by approximately 60%. At a similar weight percent, the gain in modulus observed in the present work with the addition of 1.8 wt % carbon nanotubes was only 15% and no gain in storage modulus was found for the sample filled with 0.6 wt % nanotubes. The sample with 1.8 wt % tubes also has a higher storage modulus below room temperature. Figure 1 also indicates that the addition of nanotubes caused no measurable change in the glass transition temperature as indicated by the fact that the peak in tan delta near 0 °C did not change position.

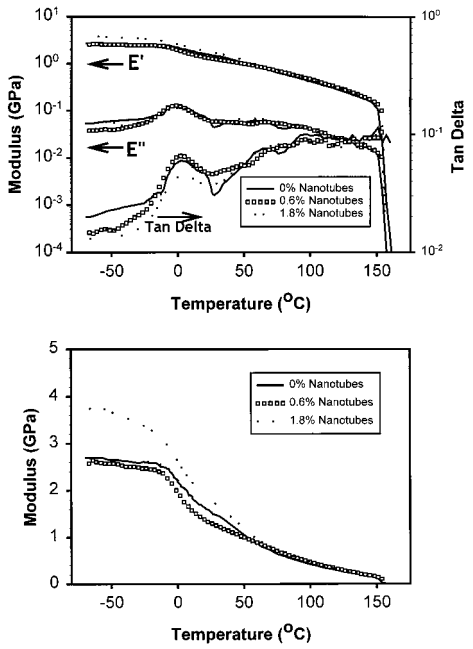

Figure 1. Dynamic mechanical spectra for filled and unfilled polypropylene. The bottom plot shows the storage modulus on a linear scale to highlight the differences in moduli at low temperatures. The difference between unfilled polypropylene and propylene filled with 0.6 wt. wt % nanotubes is statistically insignificant.

The small changes in dynamic mechanical properties could have been due to small differences in percent crystallinity; however, as will be demonstrated, percent crystallinities in nonisothermal crystallization experiments were almost the same for all samples. Hence, the difference between the sample with 1.8% nanotubes and the other two samples was due to the reinforcing effect of the nanotubes and not to simply differences in percent crystallinities.

Figure 2 represents the results from the cooling portion of nonisothermal crystallization experiments. The most obvious result is that the crystallization temperature (the temperature corresponding to the maximum of the crystallization exotherm) increases as the level of filler increases as shown in the bottom plot, indicating that nanotubes nucleate crystallization. There is a much lower impact of additional nanotubes, suggesting that almost enough nanotubes are present at 0.6 wt % to provide sufficient surface area so that crystal growth, rather than crystallite nucleation, becomes rate-limiting. In fact, for all other kinetic measurements described in this paper, little or no difference was found for the two loading levels. Another indication that carbon nanotubes nucleate crystallites is that the difference in crystallization temperatures is larger at higher cooling rates. The temperature dependence of the growth rate is almost always much greater than the temperature dependence of the nucleation rate.

The two upper portions of Figure 2 show another effect of adding nanotubes: the crystallization peak increases and

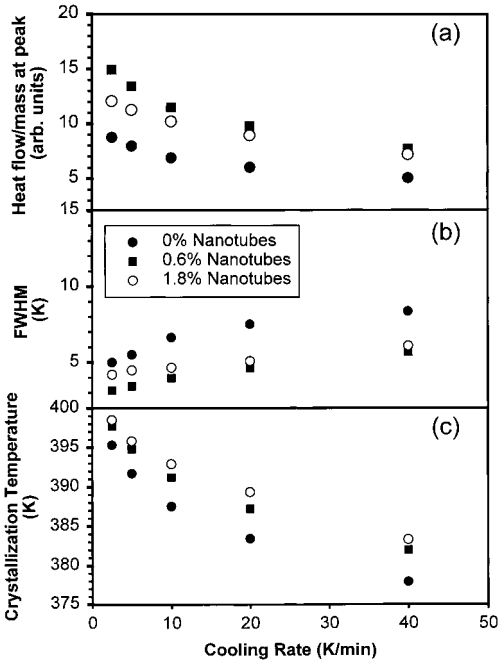

Figure 2. Results of nonisothermal crystallization kinetic studies for the cooling segment of the cool−heat cycle.

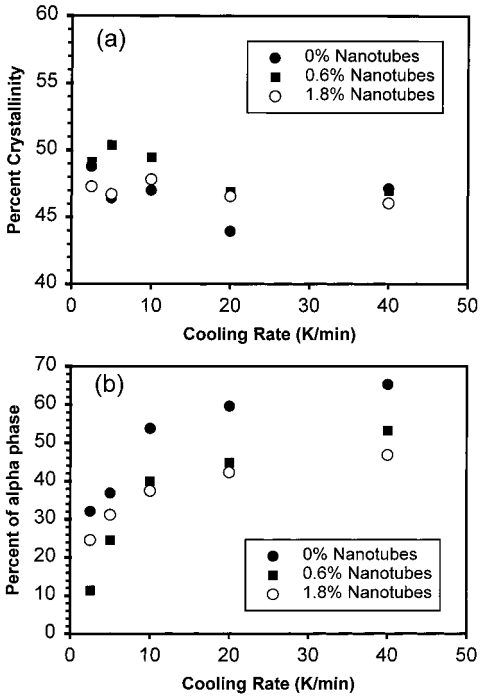

Figure 3. Results of nonisothermal crystallization kinetic studies during the heating segment of the cool−heat cycle.

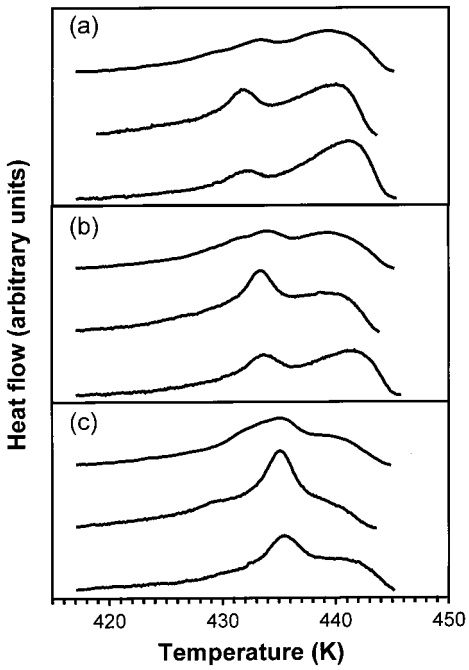

Figure 4. Baseline-subtracted DSC data from nonisothermal crystallization kinetic studies during the heating segment of the cool−heat cycle. From top to bottom, the cooling rates were 40 K/min (a), 10 K/min (b), and 2.5 K/min (c). Within each plot, the bottom line represents data from samples without nanotubes, the middle line represents data from samples with 0.6 wt % nanotubes, while the top line represents data from samples with 1.8 wt % nanotubes. The upward direction is the endothermic direction. A vertical shift has been applied to the data to enhance presentation clarity.

sharpens. The values of the full width at half-maximum (fwhm) and peak heat flow were calculated from fitting the crystallization peak using the software PeakFit from Sysstat Inc. The purpose of fitting was to obtain a more reproducible value for these two parameters, that is, better than could be obtained by inspection, so the only criterion for selecting the type of equation was that the fit was good. An asymmetric logistic function was selected and used for all peak fitting. Surprisingly, the peak sharpness for the sample with 0.6 wt % nanotubes is greater than that for the sample with 1.8 wt % nanotubes, as evidenced by a smaller fwhm as well as a higher heat flow at the peak. The product of the two parameters was roughly constant, which follows since the percent crystallinities shown in Figure 3 are roughly identical for all samples.

Figure 3 shows the results upon a subsequent heating scan after cooling at a fixed rate. The top plot shows the percent crystallinity as a function of cooling rate for the three samples. Within experimental error, no difference was found between the sample with 1.8% nanotubes and unfilled polypropylene, while at low cooling rates the percent crystallinity might be higher for the 0.6% nanotube sample, although this difference is probably not outside experimental error. A very slight increase in percent crystallinity may occur as the cooling rate lessens, but the increase is marginal if it exists at all.

The calculation of the percent crystallinity contains an error because only one enthalpy was used to calculate the percent crystallinity and two crystalline forms are clearly present. The bottom of Figure 3 shows that the fraction of the alpha phase is reduced at higher cooling rates. The fraction of the alpha phase was determined by fitting the data shown in Figure 4 to two asymmetric logistic functions using the PeakFit software. The alpha phase is the higher melting, most common monoclinic crystal structure of polypropylene. Since the enthalpy of melting for the alpha phase must be greater than that of the beta phase, the likelihood that the 0.6% nanotube sample has a slightly higher crystallization increases.

The fraction of each polymorph described in Figure 3 must be considered semiquantitative for several reasons. One reason is that recrystallization could be occurring. In other words, some of the beta phase upon melting recrystallizes and then melts as the temperature is raised further. In fact, it is not recommended to assume that bimodal melting endotherms necessarily mean polymorphic behavior; another possibility is melting of alpha crystals with small crystal thicknesses followed by recrystallization into alpha crystals with longer thicknesses followed by

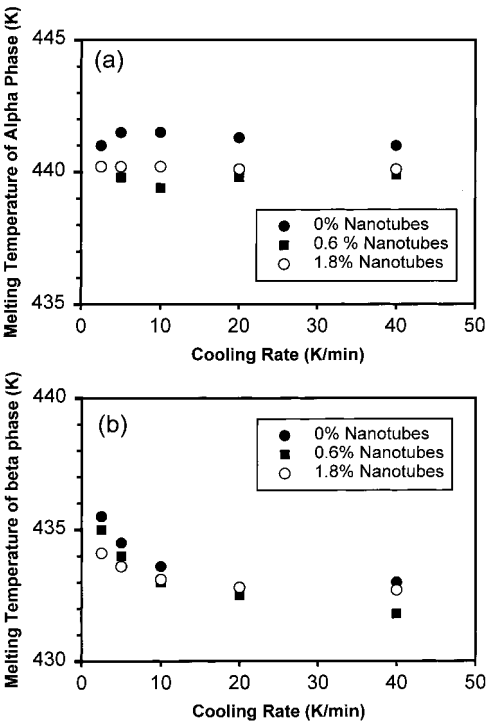

Figure 5. Melting temperatures of the two crystalline polymorphs of polypropylene from fitting of data from nonisothermal crystallization kinetic studies during the heating segment of the cool−heat cycle. The melting temperature of the alpha phase may not be entirely accurate, since an endotherm from recrystallization could be affecting the DSC trace.

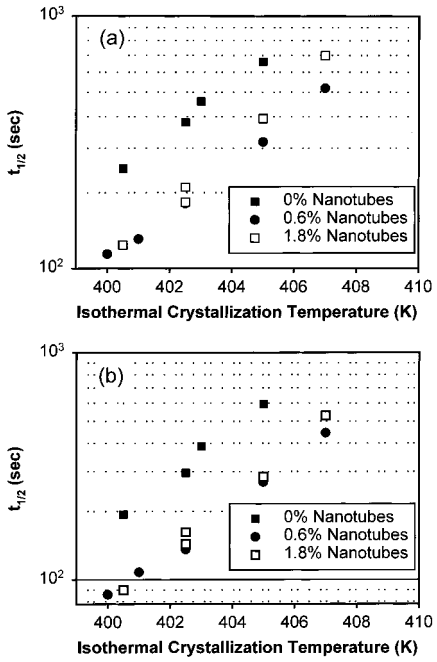

Figure 6. Crystallization halftimes from isothermal crystallization experiments. Figure 6a presents the halftime assuming that $t = 0$ was the time when cooling was initiated, while Figure 6b presents the halftime assuming that $t = 0$ was the time t_0 was determined via an Avrami fit to the data.

melting of these newly formed alpha crystallites. However, the fact that the fraction of the higher melting phase decreases with lower cooling rates and also the fact that the addition of nanotubes substantially changes the ratio of the two endothermic events mean that the DSC chromatograms shown in Figure 4 represent some sort of polymorphic behavior. However, both melting−recrystallization−melting and polymorphism could be occurring.

The fact that the fraction of alpha phase decreased at lower cooling rates is odd since the formation of thermal stresses tends to favor the formation of the beta phase and thermal stresses would be expected to be higher at higher cooling rates. Further, the addition of nanotubes caused the formation of more beta phase. This latter result is surprising, since aramid, high modulus carbon fibers, poly(ethylene terephthalate) and polyamide fibers all nucleate alpha-transcrystallinity.[9,25,26] We could find no examples in the literature where a particulate filler favored the formation of the beta-crystalline phase versus the alpha-crystalline phase. However, the growth rate of the beta crystalline phase is greater than the growth rate of the alpha phase in this temperature region,[27] so if the nanotubes nucleate both crystalline forms with equal probability then the beta form will be present in greater amounts. Very specific small molecule compounds are used to nucleate the beta phase,[22] and another possibility is that the covalently bound octadecyl chains nucleate the beta phase.

One other feature in Figure 4 deserves comment and is represented more clearly in Figure 5. A clear shift in melting temperature of the beta peak toward higher temperature occurs as the cooling rate decreased with no change in the location of the alpha peak. The shift in temperature of the beta peak cannot be considered surprising since an increasing perfection of the crystals is expected with higher temperature. This result is also consistent with the fact that the percent crystallinity of the beta phase increases with lower cooling rates, since an increased melting temperature and increased percent crystallinity typically occur together. The lack of change in the melting temperature of the alpha phase can be explained, since the fraction of the alpha phase decreased with lower cooling rates; however, the result must be considered moderately surprising. Further, if recrystallization is occurring, then possible changes in the location of the alpha peak could be masked. Unlike the percent of each polymorph, no clear difference was found in melting temperatures between the samples with and without nanotubes, except that the melting temperature of the alpha phase was slightly higher in the samples without nanotubes.

Isothermal crystallization experiments generally confirm the conclusions of the nonisothermal experiments: the addition of carbon nanotubes significantly speeds the formation and growth of crystallites. One cannot separate nucleation effects from possible increases in crystal growth rate using isothermal crystallization experiments. However, given the amount of filler present, coupled with the fact that other studies have shown that the rate of crystallite growth front movement is unaffected by fiber nucleation, by far the most likely interpretation is that increased nucleation by the nanotubes caused faster crystallization. Figure 6 shows that nanotubes reduce the crystallization halftime $t_{1/2}$; the halftime is defined as the point where the relative crystallinity reaches 50%. The top graph is simply the halftime determined with $t = 0$ as the time at which cooling began, while the bottom graph assumes $t = 0$ is τ_o. Adding nanotubes reduces the crystallization time at a given temperature by roughly a factor of 2.

Unlike the nonisothermal cooling experiments, the addition of nanotubes caused the percent crystallinity to increase at low isothermal crystallization temperatures as shown in Figure 7. The reason for this increase is not clear, but the increase was definitely statistically significant. The percent crystallinity for the samples with nanotubes seems to decrease at higher

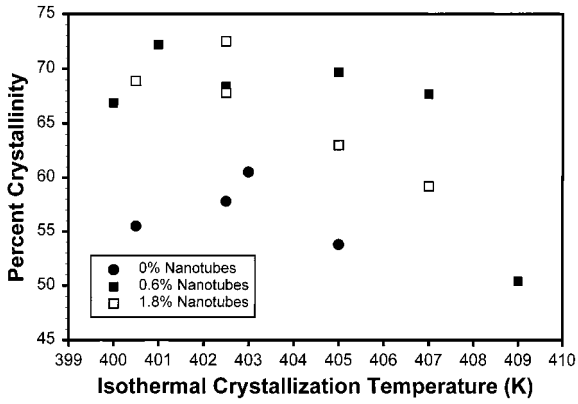

Figure 7. Percent crystallinities calculated from the magnitude of the crystallization exotherm measured during isothermal crystallization experiments.

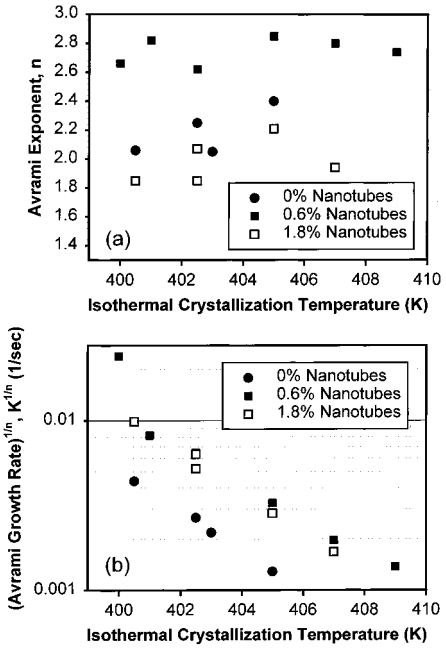

Figure 8. Avrami exponent, *n*, and Avrami growth rate, *K*, calculated from the best fit of the Avrami equation to the experimental data. $K^{1/n}$ is presented rather than *K* to force unit consistency; unit consistency is necessary to compare *K* values calculated with different *n* values.

temperatures. This conclusion should not be regarded as totally firm for the following reason. The amount of sample in the DSC pan was between 2.5 and 3.0 mg in all cases, which was previously determined to be the minimal amount required to achieve good sample−pan contact.[28] The minimum was chosen to minimize heat transfer effects. The highest temperatures in Figure 7 represent the signal-to-noise ratio limit, and in fact the data for the highest temperatures have a substantially larger error than the other data because of difficulties in precise baseline location.

The results of the Avrami fits are shown in Figure 8. As found in Figure 7, the rates of crystallization as measured by the Avrami growth rate, *K*, are much faster for the sample with nanotubes than for the sample without nanotubes. Consistent with Figure 7, no substantial difference in rate was found for the two different loading levels. Although the variance was quite large, Figure 8a also indicates that the Avrami exponent was definitely different for the sample filled with 0.6 wt % nanotubes versus the other two materials. Figure 9 shows the raw data from the experiment for two samples where the halftimes

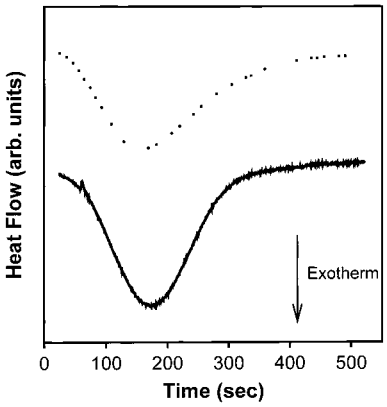

Figure 9. DSC data from isothermal crystallization kinetic studies at a crystallization temperature of 402.5 K. The solid line represents samples with 0.6 wt % nanotubes, while the dots represent data filled with 1.8 wt % nanotubes. A meaningful visual comparison could not be made for polypropylene without nanotubes because no samples were measured that had a halftime close enough to the halftimes shown in this graph. A vertical shift has been applied to the data to enhance presentation clarity.

are almost identical, and it is clear that the sample with 1.8 wt % nanotubes has a more pronounced tail at longer times than the sample with 0.6 wt % nanotubes. The results from nonisothermal crystallization experiments indicate that the split between the two polymorphs was less equal in the sample with 0.6 wt % nanotubes versus the other two polymorphs, and perhaps the differences in Avrami exponent are simply a result of this fact. A recent paper appeared in which a two-step crystallization was hypothesized and the isothermal crystallization data were fit with two separate symmetric peaks; the shape of the curve for the sample with 1.8 wt % nanotubes in Figure 9 and the curve for PP (not shown) certainly suggest that such a procedure would be justified. However, in the current case the purpose of this exercise was not clear and hence was not attempted.

We cannot determine whether transcrystallization was occurring. Transcrystallinity is an issue of degree: is the nucleation density on the filler great enough and the filler oriented enough to restrict growth transverse to the filler? Glass fibers can nucleate polypropylene crystallization without causing transcrystallinity.[29] Normally, determination of transcrystallinity is done via optical microscopy; a single fiber is placed in the polymer and the crystal growth at the fiber-matrix interface is imaged. Due to the size of the tubes, such an approach was not possible. A related question is whether transcrystallinity or fiber nucleation enhances interfacial adhesion between the filler and the fiber. The results are mixed on this question; some studies have found substantial improvements in interfacial adhesion,[4,30] while others have found no difference.[3,31] This important spatial region with respect to interfacial adhesion is almost certainly the region within approximately 1 nm of the interface, a fact noted by more than one author.[25,31] In one very interesting study, speculation focused around the orientation of the crystallites relative to the fiber and the ability of amorphous chains to occupy the space right next to the fiber.[31]

The possible role of the covalently bonded carbon chains to the nanotube cannot be overlooked. As noted earlier, sizings on glass fibers have been shown to affect the crystallization kinetics dramatically. The results of this study must be considered very specific to the nanotubes studied, both in terms of the synthetic method used and in terms of the covalently bonded molecules.

4. Conclusions

Carbon nanotubes modified with octadecylamine were mixed with polypropylene in a solvent-based process. The resulting composite had an almost negligible difference in small-strain mechanical properties. However, the introduction of carbon nanotubes changed the crystallization kinetics as measured by differential scanning calorimetry. As with certain macroscopic carbon fibers, carbon nanotubes were shown to nucleate crystallinity. The actual amount required to nucleate crystallinity was quite low; at 0.6 wt % fibers, the number of nucleation sites increased to the point where further addition produced a very small or even negligible increase in the formation of crystallites. This extremely low value confirms the obvious statement that the number of nucleated crystals is proportional to the surface area of the filler. More sophisticated means of analysis would be required to determine if the crystallites were in fact oriented normal to the nanotube surface as in transcrystallinity, and those experiments are currently under development.

Acknowledgment. Financial support for this project was provided by an NSF CAREER grant DMR-9733068 (B.P.G.). Electronic discussions with Roger Phillips of Basell Inc. were of great value. Partial support from the College of Engineering at the University of Oklahoma is also acknowledged.

References and Notes

(1) (a) Andrews, R.; Jacques, D.; Rao, A. M.; Rantell, T.; Derbyshire, F.; Chen, Y.; Chen, J.; Haddon, R. C. *Appl. Phys. Lett.* **1999**, *75*, 1329. (b) Lourie, O.; Cox, D. M.; Wagner, H. D.; *Phys. Rev. Lett.* **1998**, *81*, 1638. (c) Kearns, J. C.; Shambaugh, R. L. *J. Appl. Polym. Sci.*, accepted.

(2) Hadjieva, V. G.; Iliev, M. N.; Arepalli, S.; Nikolaev, P.; Files, B. S. *Appl. Phys. Lett.* **2001**, *78*, 3193.

(3) Dean, D. M.; Marchione, A. A.; Rebenfeld, L.; Register, R. A. *Polym. Adv. Technol.* **1999**, *10*, 655.

(4) Nielsen, A. S.; Pyrz, R. *Comput. Interface* **1999**, *6*, 467.

(5) Assouline, E.; Pohl, S.; Fulchiron, R.; Gerard, J. F.; Lustiger, A.; Wagner, H. D.; Marom, G. *Polymer* **2000**, *41*, 7843.

(6) Hegemann, H.; Veeman, W. S. *Macromol. Chem. Phys.* **1999**, *200*, 1485.

(7) Wang, C.; Liu, C. R. *Polymer* **1999**, *40*, 289.

(8) Manchado, M. A.; Biagiotti, J.; Torre, L.; Kenny, J. M. *Polym. Eng. Sci.* **2000**, *40*, 2194.

(9) Thomason, J. L.; Van Rooyen, A. A. *J. Mater. Sci.* **1992**, *27*, 889.

(10) Assouline, E.; Wachtel, E.; Grigull, S.; Lustiger, A.; Wagner, H. D.; Marom, G. *Polymer* **2001**, *42*, 6231.

(11) Wang, C.; Chen, C. C. *Polym. Bull.* **1999**, *43*, 433.

(12) Thomason, J. L.; Van Rooyen, A. A. *J. Mater. Sci.* **1992**, *27*, 897.

(13) Wang, C.; Liu, C. R. *Polymer* **1999**, *40*, 289.

(14) Dogoeva-Gaceva, G.; Janevski, A.; Mäder, E. *Polymer* **2001**, *42*, 4409.

(15) Denault, J.; Vu-Khanh, T. *Polym. Comput.* **1988**, *9*, 360.

(16) Herrera, E. J.; Balzano, L.; Borgna, A.; Alvarez, W. E.; Resasco, D. E. *J. Catal.* **2001**, *204*, 129.

(17) Alvarez, W. E.; Kitiyanan, B.; Borgna, A.; Resasco, D. E. *Carbon* **2001**, *39*, 547.

(18) Kuznetzova, A.; Mawhinney, D. B.; Naumenko, V.; Yates, J. T.; Liu, J.; Smalley, R. E. *Chem. Phys. Lett.* **2000**, *321*, 292.

(19) Mawhinney, D. B.; Naumenko, V.; Kuznetzova, A.; Yates, J. T.; Liu, J.; Smalley, R. E. *J. Am. Chem. Soc.* **2000**, *122*, 2383.

(20) (a) Chen, J.; Hamon, M.; Hu, H.; Chen, Y.; Rao, A. M.; Eklund, P. C.; Haddon, R. C. *Science* **1998**, *282*, 95. (b) Chen, J.; Rao, A. M.; Lyuksyutov, S.; Itkis, M. E.; Hamon, M. A.; Hu, H.; Cohn, R. W.; Eklund, P. C.; Colbert, D. T.; Smalley, R. E.; Haddon, R. C. *J. Phys. Chem. B* **2001**, *105*, 2525.

(21) (a) Wildoer, J. W. G.; Venema, L. C.; Rinzler, A. G.; Smalley, R. E.; Dekker C. *Nature* **1998**, *391*, 59. (b) Odom, T. W.; Huang, J.-L.; Kim, P.; Lieber, C. M. *Nature* **1998**, *391*, 62; (c) Kataura, H.; Kumazawa, Y.; Maniwa, Y.; Umezu, I.; Suzuki, S.; Ohtsuka, Y.; Achiba, Y. *Synth. Met.* **1999**, *103*, 2555.

(22) Phillips, R. A.; Wolkowicz, M. D. In *Polypropylene Handbook*; Moore, E. P., Jr., Ed.; Hanser Publishers: Munich, 1996; Chapter 3.

(23) Huda, M. N.; Dragaun, H.; Bauer, S.; Muschik, H.; Skalicky, P. *Colloid Polym. Sci.* **1985**, *263*, 737.

(24) Lozano, K.; Barrera, E. V. *J. Appl. Polym. Sci.* **2001**, *79*, 125.

(25) Varga, J.; Karger-Kocsis J. *J. Mater. Sci. Lett.* **1994**, *18*, 1069.

(26) Suhanova, T. E.; Lednicky, F.; Urban, J.; Baklagina, Y. G.; Mikhailov, G. M.; Kudryavstev V. V. *J. Mater. Sci.* **1995**, *30*, 2201.

(27) Lotz, B. *Polymer* **1998**, *39*, 4562.

(28) Grady, B. P.; Genetti, W. B.; Lamirand, R. J.; Shah, M. *Polym. Eng. Sci.* **2001**, *41*, 820.

(29) Avela, M.; Martuscelli, E.; Sellitt, C.; Garagani, E. *J. Mater. Sci.* **1987**, *22*, 3185.

(30) Folkes, M. J.; Wong, W. K. *Polymer* **1987**, *28*, 1309.

(31) Wu, C.; Chen, M.; Karger-Kocsis, J. *Polymer* **2001**, *42*, 129.